Electron paramagnetic resonance properties of n-type silicon in the intermediate impurity-concentration range*

P. R. Cullis† and J. R. Marko‡

Department of Physics, The University of British Columbia, Vancouver, B. C. V6T 1W5, Canada

(Received 23 April 1973; revised manuscript received 19 February 1974)

The EPR properties of phosphorus-doped silicon are investigated in detail for impurity concentrations $5\times10^{16}\le N_D\le 1.6\times10^{18}$ donors/cm^3 and temperatures $1.1\le T\le 35$ K. Particular care is taken to ensure that the inhomogeneously broadened spectra obtained correspond to well-defined experimental "passage cases." Rapid-passage and slow-passage spectra are converted into directly comparable "absorption envelope" forms which are convolutions of Lorentzian spin packets and Gaussian envelope functions. Spin-lattice relaxation times, spin-packet widths, and g values are presented for both the hyperfine and broad-center-line (BCL) components of the spectra. The hyperfine-line spin-packet widths exhibit a concentration dependence and have magnitudes which are larger than those expected from spin-echo measurements of T_2. A previously unreported concentration dependence is also observed for the hyperfine-line g value. Although similar g-value and spin-packet-width concentration dependences are noted for the BCL, the BCL parameters exhibit temperature dependences which are distinct from those observed for the corresponding hyperfine-line quantities. A comparison of the fractional spin susceptibility associated with the BCL and the results of a percolation calculation indicates that the BCL can be attributed to clusters of three or more interacting donor atoms. Evidence is also presented for a hyperfine-line spin-lattice relaxation process which proceeds through cross relaxation with fast relaxing cluster (BCL) centers. This process is shown to be consistent with the experimental temperature dependences of the BCL and hyperfine relaxation rates.

I. INTRODUCTION

A great amount of effort has been devoted to the study of the EPR properties of n-type silicon at low temperatures.[1] The observed characteristics of samples with relatively small impurity concentrations (N_D) are reasonably well understood in terms of the isolated-donor or pseudo-hydrogen-atom model. In this model the paramagnetic extrinsic electrons are strictly localized to a given impurity site. On the other hand, the properties of very heavily doped samples can be interpreted in terms of the formalisms usually reserved for high-density delocalized-electron "metallic" systems.[2–5]

The present work is concerned with the relatively more complex EPR properties of samples with impurity concentrations intermediate to these extremes. In the case of phosphorus-doped silicon (Si : P) this "intermediate concentration range" can be considered to include samples with $1\times10^{16}\lesssim N_D\lesssim 2\times10^{18}$ donors/cm^3. Some quantitative understanding of the EPR spectra peculiar to the lower end of this range has been obtained through the "donor-pair" approach.[6–13] This model treats the impurities as a collection of pseudohydrogen molecules, each of which consists of a pair of nearest-neighbor donors. However even at concentrations as low as $N_D=1.0\times10^{16}$ donors/cm^3, some important aspects of the EPR and optical data cannot be satisfactorily explained in these terms. Specifically, several such problems are associated with the "broad-background" EPR line [referred to as the "broad center line" (BCL) in this work], which has been directly and indirectly observed throughout the intermediate concentration range.[14–17]

Morigaki and Maekawa[17] have studied this BCL for sample impurity concentrations $N_D\ge 1.7\times10^{17}$ donors/cm^3. These authors reported asymmetries in the observed line shapes and effective g values[18] and intensities that were strong functions of impurity concentration and temperature. On the basis of these data the BCL was attributed to ferromagnetically coupled clusters of donor atoms. The electronic donor-donor interactions within each of these clusters were still assumed to be of the expected antiferromagnetic form.[8]

The Morigaki-Maekawa data and interpretation[17] are complicated by the very strong concentration dependence of the spin-lattice relaxation time T_1 in intermediately doped Si : P samples.[15] At low temperatures ($T\lesssim 10$ K) and $N_D<2\times10^{17}$ donors/cm^3 the values of T_1 are relatively large, which entails that "rapid-passage" EPR spectra are observed, whereas "slow-passage" signals are monitored for higher temperatures and/or impurity concentrations. The different characteristics of these two types of spectra have hitherto prevented observation of signals which vary in a smooth and interpretable manner over the whole of the intermediate range. The anomalous line shapes reported by Morigaki and Maekawa and, concomitantly, the lack of distinction between rapid- and slow-passage signals, introduce sufficient ambiguity into their experimental data to prevent their com-

plete acceptance. Some of the reported[17] observations can, in fact, be interpreted as due to violations of the rapid-passage conditions and/or the mixing of absorptive and dispersive responses.

In this work we have studied, under rapid- and slow-passage conditions, the inhomogeneously broadened[19] EPR responses of Si : P samples with $5\times10^{16} \leq N_D \leq 1.6\times10^{18}$ donors/cm^3 at temperatures $1.1 \leq T \leq 35$ K. Particular care was taken to ensure that all spectra observed were directly related to the so-called "absorption envelope" which represents the inhomogeneously broadened shape of the imaginary (χ'') part of the total magnetic susceptibility ($\chi = \chi' - i\chi''$) of the sample. An important result of this approach is that the envelope spectra obtained vary smoothly with N_D and can be directly compared from sample to sample over the entire intermediate concentration range. In order to facilitate interpretation, these envelope spectra are then decomposed into a small number of distinct components, each of which can be identified with a relatively well-defined subgroup of the randomly distributed donor spin system (i.e., "isolated" donors, donor pairs, donor triples, etc.). The experimentally observed behavior of the shape, intensity, and relaxation parameters associated with each of these components are used to justify this identification, evaluate previous models, and follow the spin-system dynamics.

Section II consists of a brief summary of the EPR responses obtained from inhomogeneously broadened spin systems, and is followed (Sec. III) by a description of our experimental techniques. Relaxation times, linewidth, and other data are reported in Sec. IV prior to a discussion of these results with respect to simple models in Sec. V.

II. PASSAGE CONDITIONS AND THE OBSERVED SPECTRA

A. Introduction

The most conveniently interpreted EPR signals are obtained when the spectrometer is tuned to monitor either the purely absorptive or purely dispersive responses of the paramagnetic sample. Slow-passage signals may be observed under either of these tuning conditions. Rapid-passage situations, on the other hand, require the spectrometer to be tuned to monitor dispersive responses, since the absorptive signal intensity is appreciably reduced by the saturation of the spin system. For an inhomogeneously broadened spin system as obtains in Si : P, however, both the rapid-passage dispersive and the slow-passage absorptive responses can be simply related to the absorption envelopes. We have therefore confined our experiments to such signals, and the necessary passage and spectrometer-tuning requirements are discussed below. In particular, the meaning of such parameters as the spin-packet width, and the spin-spin and spin-lattice relaxation times are considered under these circumstances and the relationship between the experimental signals and the corresponding absorption envelopes are clarified.

B. Slow passage

In the Bloch[20] phenomenological description of magnetic resonance, the slow-passage absorption-mode response of an unsaturated homogeneously broadened system is a Lorentzian profile of width $\Delta H_{\text{obs}} = 2/\gamma T_2$, where γ is the electronic gyromagnetic ratio, and T_2 is the Bloch spin-spin relaxation time. We consider the slow-passage response of an inhomogeneously broadened system to be described by the Portis "spin-packet" approach,[21] as extended by Castner.[22] The net profile observed is then thought of as a convolution of independent, homogeneously broadened Lorentzian spin-packet contributions of width ΔH_p, with a distribution function of width ΔH_G. Most commonly encountered sources of inhomogeneous broadening elicit a Gaussian distribution function[23] and the resulting absorption envelope is commonly designated as a Voigt profile.[24,25] This envelope has, respectively, Gaussian and Lorentzian character in the $\Delta H_p \ll \Delta H_G$ and $\Delta H_p \gg \Delta H_G$ limits. If magnetic field modulation of small enough amplitude is applied, the first-harmonic signal monitored is the derivative of this absorption envelope.

The spin-packet concept, which is central to this approach, has no universally accepted definition. In the original Portis formulation of inhomogeneous broadening,[21] the utility of the spin packet was based on the assumption that spins whose local fields differ by more than a packet width can be independently treated. The interaction (or spectral diffusion) between spin packets was also neglected in the Castner theory[22] of the saturation behavior of inhomogeneously broadened lines. More recently, however, Wolf[26] and Clough and Scott[27] have included spectral diffusion in their calculations only to obtain saturation behavior identical to that of Castner. Although Clough and Scott[27] consider this agreement to be accidental, we believe that the two approaches may be reconciled if the spin packet is viewed in different terms. We follow Klauder and Anderson,[28] who suggest that the group of constituent spins in a spin packet takes on a "quasiparticle" status. It is then the lifetime of these "effective" spins that becomes shortened (with accompanying increase of ΔH_p) by the mutual spin-spin flips inherent to spectral diffusion. The Castner formulation will then automatically include situations where spectral diffusion occurs if the resonance line shape of each of these effective spins (or spin

packets) is Lorentzian. Calculation has shown this to be the case for a randomly distributed spin system with dipolar coupling,[29] and simple arguments show a similar result when the interactions are dominated by exchange.[30]

In this work we take the Klauder-Anderson[28] view of the spin packet and, further, will assume that the packet spin-spin relaxation time in the presence of spectral diffusion still satisfies the usual expression:

$$2/T_2 = \gamma \Delta H_p \ . \tag{1}$$

This definition is consistent with the analogous relationship for homogeneously broad lines (i.e., $2/T_2 = \gamma \Delta H_{\text{obs}}$) since, as shown in the Appendix, $\Delta H_p = \Delta H_{\text{obs}}$ in the rapid-spectral-diffusion or homogeneous limit. Spin-lattice relaxation processes, on the other hand, must be treated slightly more carefully, as the net rates of such processes are dependent upon the degree of saturation when spectral diffusion mechanisms are present. It is convenient to employ the results of Clough and Scott,[27] in which a parameter, $1/T_3$, is used to describe the rate at which the spin system approaches internal thermal equilibrium (or restablishes a "spin temperature") through spectral diffusion. If the system is saturated (as under rapid passage) and $T_3 \ll T_1$, the spin system will assume a spin temperature in a time on the order of T_3, from which it will approach the lattice temperature with the time constant T_1, after the microwave radiation is turned off. The spin-lattice relaxation time is then given by T_1. If, on the other hand, the spin system is not saturated (slow passage), and $T_3 \ll T_1$, the spin temperature and lattice temperature are effectively the same, even in the presence of microwave radiation. Thus the effective spin-lattice relaxation time would be given by T_3. Clough and Scott obtain $T_3 = (T_1 T_2/a)^{1/2}$, where a is their version of an "inhomogeneity parameter." Our major assumption is that we can identify their a with that of Castner ($a = 0.832\ \Delta H_p/\Delta H_G$). This association is nonrigorous, but, as pointed out by Clough and Scott, a does take the same numerical values in both theories for similar "saturation curves." The net relaxation rate of a spin in the presence of spectral diffusion for slow-passage (nonsaturating) conditions can then be written as $1/\tau$, where

$$\frac{1}{\tau} = \frac{1}{T_1} + \frac{1}{T_3} \ . \tag{2}$$

C. Rapid passage

A lucid and general discussion of the rapid-passage EPR responses of inhomogeneously broadened systems has been offered by Portis.[31] The signals observed in the dispersive mode of a spectrometer employing audio-frequency magnetic field modulation and phase-sensitive first-harmonic detection are of particular interest. We present, in Table I, a compilation of the basic rapid-passage cases and the corresponding signal line shapes, amplitudes, and phases (with respect to the modulated magnetic field). The symbols used are of conventional form. Those not previously defined include H_m and ω_m, which represent the amplitude and angular frequency, respectively, of the modulated magnetic field. The amplitude of the microwave-frequency magnetic field is given by H_1.

Table I is a slightly modified version of the previous compilation of Portis.[31] Our alterations of, and comments on, the original formulation are detailed below.

(i) The Portis formulation employs a spin-relaxation time τ which has no clear interpretation in terms of T_1 or T_2. It can be shown,[24] however, that this τ may be replaced by the spin-lattice relaxation time T_1 (as we have done), if this spin-lattice relaxation time is the same in the rotating and laboratory frames of reference. As noted by Clough and Scott,[27] this equivalence of the two T_1's can be justified for rapid-passage EPR situations, similar to those encountered in the present work, where spin-spin interactions are sufficiently small to result in an inhomogeneously broadened line.

(ii) We have found, in the Si : P system, that the passage condition $T_1\, dH_0/dt < H_m$ common to the original Portis cases 2A and 2B is overly restrictive. Experimentally it was found to be necessary to violate this condition by at least two orders of magnitude before line-shape distortions appeared which could be associated with those expected in the $T_1\, dH_0/dt > H_m$ limit (case 4). This behavior is in accord with the observations of Feher[19] for the situation in which the inequalities $T_1\, dH_0/dt$, $\Delta H_G > H_m$ are satisfied. A possible explanation of these results is suggested by the "loss-of-magnetization" phenomena observed by Feher.[19] The condition $T_1\, dH_0/dt < H_m$ requires that the large magnetic field H_0 (which is swept linearly with time) remains at a given value of H_0, sampling spin packets within the range $H_0 \pm H_m$, for a time on the order of T_1. This presumably guarantees that a steady-state response is obtained. If the loss-of-magnetization phenomenon occurs this steady state could be achieved in a time appreciably less than T_1, which would account for the insensitivity of the case 2A and 2B signals to the inequality in question.

(iii) As noted in Table I we have divided passage case 2B into two parts, according to whether $\omega_m T_1$ is greater or less than H_1/H_m. Portis[31] originally considered only the situation where $\omega_m T_1 > H_1/H_m$,

TABLE I. Rapid-passage conditions and the corresponding signal responses in the dispersion mode obtained from inhomogeneously broadened systems. General conditions: $H_1 > \Delta H_p$, $H_1 H_m < \Delta H_G$, $dH_0/dt < \omega_m \Delta H$, $\gamma H_1 T_1 > 1$ (saturation condition), dH_0/dt, $\omega_m H_m < \gamma H_1^2$ (adiabatic condition).

Case	Passage conditions			Amplitude of first harmonic χ'	Line shape of first harmonic χ'	Phase, relative to modulation
1	$\omega_m T_1 < \frac{H_1}{\Delta H} < 1$	$H_m < \frac{H_1}{\omega_m T_1}$	$T_1 \frac{dH_0}{dt} < H_1$	$\chi_0 \frac{H}{\Delta H_{pp}} \frac{H_m}{\Delta H_{pp}}$	dispersion derivative	0
2A	$\omega_m T_1 < 1$	$H_m < H_1$	$T_1 \frac{dH_0}{dt} < H_1$	$\chi_0 \frac{H}{\Delta H_G} \omega_m T_1 \frac{H_m}{H_1}$	absorption envelope	$\pi/2$
2B	$\frac{H_1}{H_m} < \omega_m T_1 < 1$	$H_m > H_1$	$\frac{dH_0}{dt} < \omega_m H_m$	$\chi_0 \frac{H}{\Delta H_G} \ln\left(\frac{2H_m \omega_m T_1}{H_1}\right)$	absorption envelope	$\pi/2$
	$\omega_m T_1 < \frac{H_1}{H_m}$	$H_m > H_1$	$\frac{dH_0}{dt} < \omega_m H_m$	$\chi_0 \frac{H}{\Delta H_G} \frac{2}{\pi} \omega_m T_1 \frac{H_m}{H_1}$	absorption envelope	$\pi/2$
3A	$\omega_m T_1 > 1$	$H_m < H_1$	$T_1 \frac{dH_0}{dt} < H_1$	$\chi_0 \Delta \frac{H}{H_G} \frac{H_m}{H_1}$	absorption envelope	π
3B	$\omega_m T_1 > 1$	$H_m > H_1$	$T_1 \frac{dH_0}{dt} < H_m$	$\chi_0 \frac{H}{\Delta H_G} \ln\left(\frac{2H_m}{H_1}\right)$	broadened absorption envelope	π
4	$\omega_m T_1 > 1$	...	$T_1 \frac{dH_0}{dt} > H_1, H_m$	$\pm \chi_0 \frac{H}{\Delta H_{pp}} \frac{H_m}{\Delta H_G} \ln\left(\frac{2\Delta H_G}{H_1}\right)$	absorption derivative	Sign changes with reversal of travel.

realizing that if this condition were not obeyed the rapid-passage saturation and/or adiabatic condition would be violated. As pointed out by Bugai,[32] however, violation of the adiabatic condition is equivalent to violation of the saturation requirement from the passage-condition point of view. The slow-passage response produced by such a violation is invariably *in phase* with the modulated magnetic field. Signals corresponding to case 2B are, however, observed to be $\pi/2$ out of phase with the modulated field. A phase-sensitive detector tuned to monitor such signals will therefore be insensitive to violations of the saturation condition as manifested by slow-passage effects. We therefore calculated the result for $\omega_m T_1 < H_1/H_m$, and obtained a response similar (except for a factor $2/\pi$) to that of case 2A.

Three further features of the case 2A and 2B results are worthy of special note. First, the signal height undergoes a transition from a linear to a logarithmic dependence on H_m (corresponding to a transition from case 2A to case 2B) when $H_m \simeq \omega_m T_1 H_1$. This transition point is to be contrasted to the $H_m = H_1$ dividing line between cases 3A and 3B. Second, the linear relation that exists between the signal amplitude and T_1 for the $\omega_m T_1 < H_1/H_m$ section of case 2B offers a simple and direct way of measuring relative spin-lattice relaxation times, as a function of temperature, for a given sample. Finally, if $H_m \ll \Delta H_G$, the $\omega_m T_1 < 1$ in-quadrature signals are *not* broadened by H_1 effects as are the $\omega_m T_1 > 1$ π-out-of-phase signals corresponding to cases 3A and 3B.[19,21]

(iv) It can be shown[24] (using the Klauder-Anderson concept of the spin packet) that the Portis[31] formulation is strictly correct only when $H_1 > \Delta H_p$. In situations where $H_1 < \Delta H_p$ the passage cases established by Portis become modified to the extent that H_1 is replaced by ΔH_p. This substitution has two consequences. First, the signal envelope can be regarded as a convolution of spin-packet contributions of width ΔH_p with a Gaussian distribution function, and thus is directly comparable to slow-passage absorption-envelope signals. Second, the transition from case 3A to case 3B noted in point (iii) occurs when $H_m \simeq \Delta H$. The change from a linear to a logarithmic dependence of the signal amplitude on H_m can therefore be used to measure ΔH_p in such situations.

D. Absorption envelope and the slow- and rapid-passage responses of intermediately doped Si:P

One of the main results of the Portis[31] work is the unambiguous relationship established between the rapid-passage dispersion-mode EPR signals and the absorption envelope. This means that for $T \lesssim 10$ K and $N_D \lesssim 2\times10^{17}$ donors/cm^3 we can observe (using magnetic field modulation) EPR signals which represent the undifferentiated absorptive (χ'') component of the complex magnetic susceptibility of the sample when $H_1 < \Delta H_p$. At high temperatures and/or concentrations the slow-passage absorption-mode response is proportional to the first derivative of this absorptive component ($d\chi''/dH$) if magnetic field modulation is employed. Integration of these derivative spectra therefore gives representations of $\chi''(H)$ which can be direct-

ly compared to the rapid-passage signals obtained at lower impurity concentrations and/or temperatures.

III. EXPERIMENTAL APPARATUS AND TECHNIQUES

A. Apparatus and general techniques

Our measurements were made using a standard x-band reflection-type spectrometer which employed "narrow-band" phase-sensitive lock-in detection to the variable-frequency ($50 \leq \omega_m/2\pi \leq 5\times10^4$ Hz) modulated magnetic field. A constant microwave power level at the crystal detector, independent of the power incident on the resonant cavity, was required for uniform sensitivity on our slow-passage saturation experiments. This was provided by a "bucking-arm" arrangement described by Wilmshurst.[33] A TE_{102} brass sample cavity, resonant at $\simeq 9.1$ GHz, was used which had a loaded Q of approximately 4000 at helium temperatures, allowing microwave magnetic fields of up to 1-G (peak to peak) amplitude at maximum klystron power (55 mW). Critical coupling of the sample cavity was achieved by an externally adjustable variable coupler. The experimental methods used for temperature measurement and control have been described in a previous publication.[5]

Our rapid-passage experiments, as previously noted, required observation in the dispersion mode of the spectrometer as the absorptive component of the signal is saturated. In such situations the klystron frequency was "locked" (via a standard automatic-frequency-control unit) to an adjustable wavemeter. The wavemeter frequency was set to correspond to a point approximately one-third to one-half way up the "dip" produced in the reflected klystron mode by the cavity absorption. Slow-passage experiments, on the other hand, were generally made in the absorption mode of the spectrometer, where the klystron frequency was locked to that of the resonant sample cavity. Distortions due to the "mixing in" of dispersive responses were minimized by this process.

The EPR signals obtained were recorded both graphically and digitally. LiF : Li (Ref. 4) and proton NMR marker techniques were used to establish the g values and linewidths associated with the experimental spectra. In general, we attempted to confine our measurements to signals corresponding to one of the well-established passage cases.

Four methods of measuring the phenomenological spin relaxation times T_1 and T_2 were employed. Three of these are applicable to rapid-passage EPR signals, while the fourth is strictly a slow-passage technique. The methods are detailed in the following subsections.

B. Rapid-passage recovery method of measuring T_1

In our version of this standard technique,[34] the usual linear sweep of the static field H_0 was replaced by a low-frequency (0.01 to 1 Hz) triangular or sawtooth modulation of period T_m. The experimental situation is depicted in Fig. 1 together with sketches of the observed signals as a function of time. As noted by Feher, on each single rapid passage through the line, the magnetization observed is appreciably reduced. In our situation, during the time $T_M/2$, the line is actually traversed many times owing to the audio-frequency magnetic field modulation, and we may therefore expect the magnetization to be very appreciably reduced by each single low-frequency pass through the line. If the magnetization is totally destroyed (saturated) during each such pass through the line, the ratio of two successive steady-state signal amplitudes S may be written as

$$R(T_M, \Delta t_1) = \frac{S(\Delta t_1)}{S(T_M - \Delta t_1)} = \frac{1 - e^{-\Delta t_1/T_1}}{1 - e^{-(T_M - \Delta t_1)/T_1}} , \quad (3)$$

assuming an exponential spin-lattice relaxation process. It is easily shown that incomplete saturation during each passage through the line leads to reduced values of R for $\Delta t_1 > T_M/2$. To allow for this, we increased H_1 and/or the sinusoidal modulation frequency ω_m for a given Δt_1 until a maximum ratio $R(T_M, \Delta t_1)$ was achieved. The ratio's R were measured for various Δt_1's by simply adjusting the mean static field value H_0. Equation (3) could then be fitted, using T_1 as the adjustable parameter, to the experimental curve of R vs Δt_1. It was observed that the most accurate estimates of T_1 were obtained when $T_M \simeq 4T_1$. Owing to response-time limitations, this method was confined to situations where $T_1 \gtrsim 0.5$ sec.

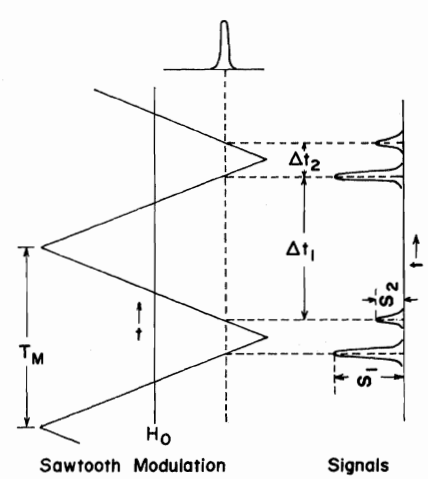

FIG. 1. Schematic representation of the recovery technique used to measure T_1 in rapid-passage situations.

C. Rapid-passage phase method of determining T_1

It can be easily shown from the results of Portis[31] that rapid-passage signals observed when $H_1 > H_m, \Delta H_p$ have maximum amplitude at a lock-in amplifier phase setting ϕ_{RP} such that

$$\phi_{RP} - \phi_0 = \theta - \pi \quad , \tag{4}$$

where $\theta = \cot^{-1}(\omega_m T_1)$, $0 \leq \theta \leq \pi/2$, and ϕ_0 is the maximum-amplitude phase setting for signals "in phase" with the modulation. The phases corresponding to cases 2A and 3A of Table I represent the $\omega_m T_1 \ll 1$ and $\omega_m T_1 \gg 1$ limits of Eq. (4), respectively.

In this work the phase setting ϕ_0 was determined by introducing an additional Si : P sample ($N_D = 2\times 10^{18}$ donors/cm^3) into the cavity. This sample exhibited only slow-passage, in-phase signals, which therefore have maximum amplitudes at phase settings $\phi_{SP} = \phi_0 + n\pi$, where $n = \pm 1, \pm 2$, etc. The phase setting ϕ_{RP} corresponding to maximum amplitude of the rapid-passage signal can then be measured, and the phase difference between the two signals written as

$$\phi_{RP} - \phi_0 - n\pi = \phi_{RP} - \phi_0 + \pi = \theta \quad , \tag{5}$$

where we choose $n = -1$ and employ Eq. (4). Experimentally, to calculate θ for a particular ω_m, the phase difference $\phi_{RP} - \phi_{SP}$ is measured and multiples of π added to or subtracted from it until the angle θ (between 0 and $\pi/2$) is obtained. The T_1 of the sample is determined from the slope of the plot $\cot\theta$ vs ω_m. With the available range of modulation frequencies, it was possible to make relaxation-time measurements over the interval $10^{-2} \leq T_1 \leq 10^{-6}$ sec.

D. Rapid-passage "modulation-amplitude" method for measuring ΔH_P

This technique was discussed in Sec. II C in connection with the transition from case 3A to 3B of Table I (as H_m is increased) when $H_1 < \Delta H_P$. The breakdown of the linear relationship between H_m and the signal amplitude when $H_m \simeq H_P$ gives a rough measure of ΔH_P. Experimentally, we reduced H_1 until the values of ΔH_P obtained became independent of any further decrease of H_1. Otherwise this technique would serve only to measure H_1.

E. Slow-passage saturation method for measuring T_1 and ΔH_P

We used a slight modification[35] of a method detailed by Castner,[22] which entails measurement of the relative absorption-envelope signal intensity $S(H_0)$ at the center of the (integrated) slow-passage EPR line. The resulting "saturation curves," $S(H_0, H_1)$ vs H_1, yield values of the spin-packet width ΔH_P and the relaxation-time parameter $(T_1T_2)^{1/2}$, assuming a sufficient range of microwave wave power is available. If Eq. (1) holds, T_1 and T_2 are determined by this method. It should be realized, however, that the values of T_1 thus obtained are inherently more uncertain than those obtained for ΔH_P, owing to the fact that the determination of $(T_1T_2)^{1/2}$ requires an absolute measurement of the microwave magnetic field H_1.

IV. EXPERIMENTAL RESULTS

A. General description of the observed spectra

We present in Fig. 2 a series of absorption-envelope signals, obtained at 1.2 K, which illustrate the gross concentration dependence of the EPR spectra of Si : P samples in the intermediate range. The traces given for samples with impurity concentrations $N_D \geq 2.2\times 10^{17}$ donors/cm^3 were obtained by a computer integration of the experimental slow-passage absorption derivative responses. As discussed in Sec. II D, these curves can be directly compared with the rapid-passage dispersion-mode signals obtained for samples with smaller impurity concentrations ($N_D \leq 1.2\times 10^{17}$ donors/cm^3).

We observe that these envelope spectra may be decomposed into three major components—the two "hyperfine" lines, the central "pair" line, and the "broad center line" (BCL). This decomposition ignores the distinct lines which arise from clusters of three or four donors. These lines are small features of the observed spectra, however, and can be accounted for in a simple manner. The characteristics of the three main EPR components are discussed below.

(i) Hyperfine lines: These two lines are the only signals directly observable for samples with $N_D \leq 1\times 10^{16}$ donors/cm^3 and for $T \leq 30$ K. They are centered at the resonant magnetic fields H^{hf}, where

$$H^{hf} = \frac{1}{g_H \mu_B} \left(\hbar\omega \pm \tfrac{1}{2}A - \frac{A^2 \hbar}{2\omega} \right) \quad . \tag{6}$$

In this expression μ_B represents the Bohr magneton, $\hbar$ is Planck's constant divided by 2π, and ω is the angular microwave frequency. The donor-electron g value and hyperfine constant are denoted by g_H and A, respectively, and the EPR lines are regarded as Voigt profiles in both the rapid- and slow-passage regimes (as long as $H_1 \ll \Delta H_P^H$). The hyperfine lines exhibit a Curie-law susceptibility[36] and their intensity is observed to decrease relative to that of the BCL as the impurity concentration is increased from $N_D \approx 5\times 10^{16}$ donors/cm^3.

(ii) Central pair line: At 1.1 K this discrete line appears approximately 0.5 G below the midway point between the two hyperfine lines for samples with $3\times 10^{16} \leq N_D \leq 1.2\times 10^{17}$ donors/cm^3. This small shift has been interpreted as evidence for the fact that this line originates from completely delocalized electrons.[37] The presently available

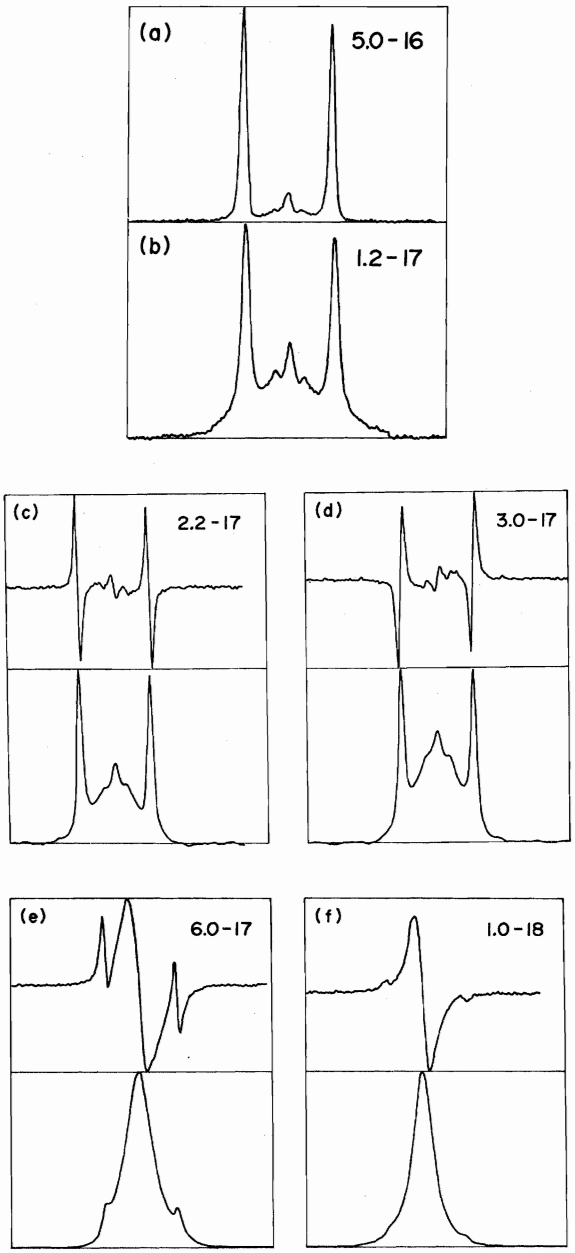

FIG. 2. Absorption-envelope spectra for intermediately doped Si : P sample at 1.2 K. The sample number is given in the upper right-hand corner of each figure. (a) and (b) represent rapid-passage dispersion-mode responses. (c)–(f) give the slow-passage absorption-mode derivative signals and the corresponding (integrated) absorption-envelope spectra. All spectra are plotted on the same scale, the full sweep width being 150 G.

transport and EPR data do not, however, lend any support to this hypothesis. The position and other characteristics of this resonance are very satisfactorily explained if one assumes that it arises from the $m_I = 0$ (where m_I is the z component of the total nuclear spin) donor-pair transition, provided the energy levels are calculated to second order.[38] The shape and half-width of this line are not noticeably different from the hyperfine line values. Its intensity, relative to that of other components, is temperature dependent and has been discussed elsewhere.[39] Since these experimental properties are all fairly consistent with the predictions of the pair model, this line did not receive any further detailed investigation in the work presently under discussion.

(iii) Broad center line (BCL): As seen in Fig. 2, a broad EPR line, underlying the other relatively discrete spectral components, was directly observed for samples with $N_D \geq 5\times 10^{16}$ donors/cm^3. The BCL shapes were always consistent with the Voigt profile. We describe the position of this line by an effective g value g_B, which is defined so that the BCL envelope has its maximum amplitude at a field

$$H^B = \omega\hbar/g_B\mu_B \quad . \tag{7}$$

It was found that g_B always exceeds g_H, and exhibits a temperature dependence which is in qualitative agreement with the previously reported 46-GHz results.[17] The disappearance of the BCL for samples with $N_D \lesssim 1.5\times 10^{17}$ donors/cm^3 and $T > 4.2$ K can be attributed to rapid-passage effects,[24] and to the observation of slow-passage absorption derivative spectra without subsequent integration. The experimental behavior of this line strongly suggests that it is the low-concentration precursor of the single spectral line[5] observed in heavily doped samples ($N_D \gtrsim 1.5\times 10^{18}$ donors/cm^3).

In the following subsections we present and briefly discuss the experimental data obtained for the hyperfine and BCL spectral components.

B. Experimental data on the hyperfine lines

(i) Experimental observability: The two hyperfine lines were observed in samples with impurity concentrations $N_D \leq 1.0\times 10^{18}$ donors/cm^3. For samples with $N_D \leq 1.2\times 10^{17}$ donors/cm^3, these lines remained in evidence at temperatures up to 35 K. As this upper temperature limit is approached, the hyperfine lines simultaneously broaden, move together, and subsequently disappear. This behavior is similar to that reported by Lépine[40] for slightly less concentrated samples. The Curie-law susceptibility of these lines and the increasing importance of the BCL combine to limit their observability to $T \lesssim 30$ K in more highly concentrated ($N_D \gtrsim 2.2\times 10^{17}$ donors/cm^3) samples. This maximum temperature at which the hyperfine lines may be detected falls to approximately 10 K as N_D is further increased to $\simeq 1.0\times 10^{18}$ donors/cm^3.

(ii) Hyperfine constant and g values: The splitting between the hyperfine lines ($A = 41.6 \pm 0.3$ Oe)

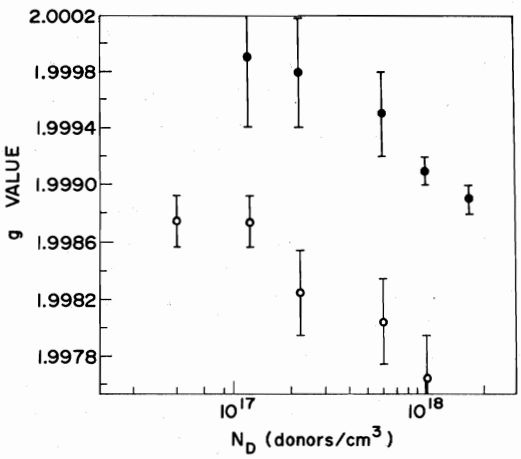

FIG. 3. Hyperfine-line g values (open circle) and BCL (closed circle) as a function of donor concentration ($T = 1.2$ K).

was observed to be independent of the impurity concentration.[41] We detected, however, a previously unreported concentration dependence of the hyperfine-line g value (g_H) appropriate to Eq. (8). Our experimental values of g_H are plotted as a function of N_D in Fig. 3. The values of g_H at the low end of our impurity concentration range agree (within experimental error) with the value reported by Feher.[19] However, it is seen that this experimental quantity decreases smoothly with increasing N_D in the upper half of the intermediate concentration range. Although the accuracy of our measurements decrease with rising temperature, no significant temperature dependence of g_H was observed.

(iii) Spin-packet widths: Our measured values of the hyperfine-line spin-packet widths (ΔH_P^H) are shown as a function of N_D in Fig. 4. These widths were obtained by either the modulation-amplitude or slow-passage saturation techniques depending upon the magnitudes of the spin-relaxation times. The observed values of ΔH_P^H were independent of temperature (up to at least 10 K) in all samples. As noted in Fig. 4, our data indicate that ΔH_P^H is proportional to the second or third power of the impurity concentration over most of the intermediate range. Both this concentration dependence and the experimental spin-packet-width magnitudes are inconsistent with earlier spin-echo measurements[42] of ΔH_P^H if the observed echo decay times are assumed equal to T_2. Finally it should be noted that ΔH_P^H was equal to the observed hyperfine linewidths for samples with $N_D \gtrsim 6\times 10^{17}$ donors/cm^3. In the latter cases, the measured values of a were greater than 1, and the nearly Lorentzian lines can be considered to be homogeneously broadened.

(iv) T_1 measurements: The experimental spin-lattice relaxation times (T_1^H) associated with the hyperfine lines are presented in Fig. 5. These results were obtained using the rapid-passage re-

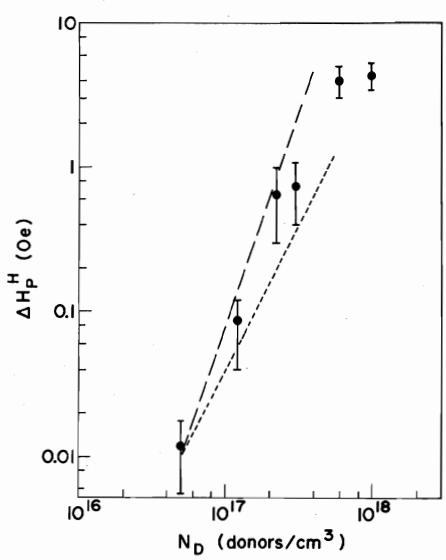

FIG. 4. Hyperfine-line spin-packet widths at 1.2 K as a function of impurity concentration. The small-dash line illustrates an N_D^2 dependence, whereas the large-dash line illustrates an N_D^3 dependence.

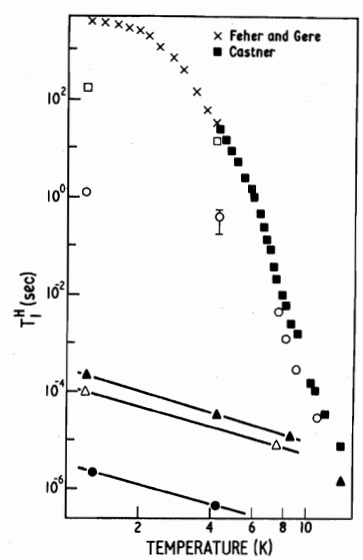

FIG. 5. Hyperfine-line spin-lattice relaxation times as a function of temperature for intermediately doped Si : P samples. Included in this figure are the results of Refs. 15 and 43 for a sample with $N_D = 1.0\times 10^{16}$ donors/cm^3. Data are plotted for sample 5.0-16 (open square), sample 1.2-17 (open circle), sample 2.2-17 (closed triangle), sample 3.0-17 (open triangle), and sample 6.0-17 (closed circle).

covery and phase methods for samples with $N_D \leq 1.2\times10^{17}$ donors/cm^3, and through the slow-passage saturation technique for more highly concentrated materials. The relaxation times for sample 2.2-17 were such that both slow- and rapid-passage signals could be observed for temperatures $T \lesssim 10$ K, and thus allowed the use of both the phase and saturation methods in this sample. It was found that these rapid- and slow-passage techniques preferentially sample the slowest and fastest relaxing spins, respectively, in the microscopically inhomogeneous sample.[9] Some ambiguity does exist, therefore, in the quoted values of T_1^H for sample 2.2-17. For consistency we have chosen to use only the slow-passage values for samples with $N_D \geq 2.2\times10^{17}$ donors/cm^3.

Figure 5 also includes T_1^H data obtained by Feher and Gere[15] and Castner[43] for a sample with $N_D \simeq 1\times10^{16}$ donors/cm^3 in which the relaxation is dominated by intrinsic (concentration independent) spin-lattice relaxation mechanisms. It can be observed that extrinsic (concentration dependent) processes control the relaxation rate at all experimental temperatures in samples with $N_D \geq 2.2\times10^{17}$ donors/cm^3. Further, the temperature dependence of this extrinsic mechanism would appear to be described by the relation[44]

$$T_1^H \propto T^{-n}, \tag{8}$$

where $n = 1.5 \pm 0.2$. A similar temperature dependence for the extrinsic process has been previously observed[45] in samples at least as dilute as $N_D = 3.9\times10^{16}$ donors/cm^3. The concentration-dependent mechanisms remain dominant over intrinsic processes for temperatures $T < T_m$, where T_m is a maximum temperature which increases with N_D.

C. Experimental data on the broad center line (BCL)

(i) BCL line shape: As indicated in Sec. IV A our experimental absorption-envelope spectra could always be decomposed in terms of symmetric, inhomogeneously broadened, broad center lines of the Voigt-profile form. A similar procedure could not be applied to slow-passage dispersion-mode $d\chi'/dH$ signals, because, aside from other factors, it proved extremely difficult to totally exclude "mixed-in" absorptive components. The latter signal contributions introduce asymmetry into the experimental line shapes and can be shown[46] to be responsible for the distortions of the type observed by Morigaki and Maekawa.[17] In the slow-passage absorption mode any dispersive $d\chi'/dH$ components can be effectively eliminated by electronically locking the klystron frequency to that of the sample cavity.

(ii) g values: Our experimental values of g_B, obtained at 1.2 K, are given in Fig. 3. These values tend smoothly with increasing N_D toward the so-called "conduction-electron" g value $g_e = 1.9988$. This behavior of g_B mirrors the concentration dependence of g_H noted previously, and it can be seen that $g_B - g_H = 0.0014 \pm 0.0002$ for $N_D \geq 1.2\times10^{17}$ donors/cm^3. This value of $g_B - g_H$ is consistent with the field shift of the BCL (relative to the center of the hyperfine-line pattern) previously reported by Morigaki and Maekawa.[17] Absolute field positions were not measured in this earlier work, however, and the possibility of a concentration dependence in g_H was not examined.

A temperature dependence of g_B was observed in our work, and is illustrated in Fig. 6 for sample 6.0-17. The values of g_B decrease with rising temperature, approaching the conduction-electron g value at higher temperatures. This dependence is again in rough accord with the results of Morigaki and Maekawa.[47] It is interesting to note, however, that in more concentrated samples ($N_D \gtrsim 2\times10^{17}$ donors/cm^3) the temperature independence of g_H results in a significant deviation, $g_B - g_H$, at all experimental temperatures.

(iii) BCL widths and spin-packet widths: The observed envelope linewidths ($\Delta H_{\rm obs}^B$) of the BCL are plotted as functions of concentration and temperature in Figs. 7 and 8, respectively. It can be observed that the BCL narrows appreciably with increase of temperature or impurity concentration. The BCL spin-packet widths (ΔH_P^B) for samples 2.2-17 and 3.0-17, as obtained by the saturation technique, are plotted as a function of temperature in Fig. 9. The interesting feature of these results is that as the over-all linewidth $\Delta H_{\rm obs}^B$ decreases with rising temperature, an increase is noted in the packet linewidths ΔH_P^B. This temperature dependence was not restricted to slow-passage situations, as similar behavior was indirectly observed in samples 5.0-16 and 1.2-17 via a rapid-

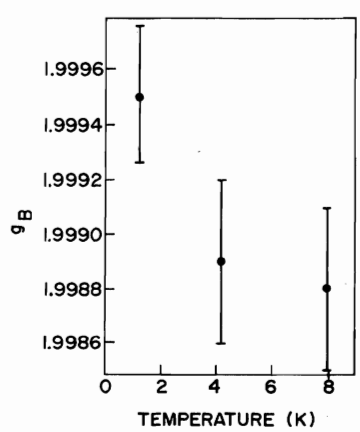

FIG. 6. Experimental temperature dependence of the BCL g value for sample 6.0-17.

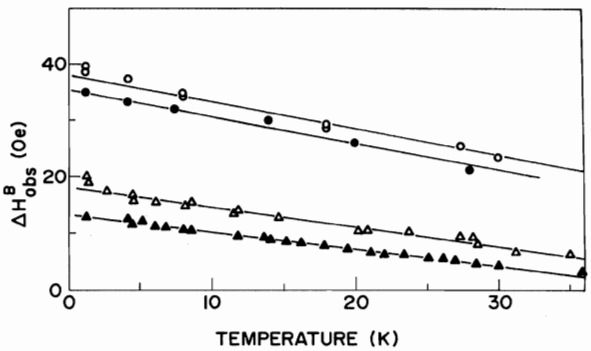

FIG. 7. BCL linewidths as a function of temperature. Data are plotted for sample 2.2-17 (open circle), sample 3.0-17 (closed circle), sample 6.0-17 (open triangle), and sample 1.0-18 (closed triangle).

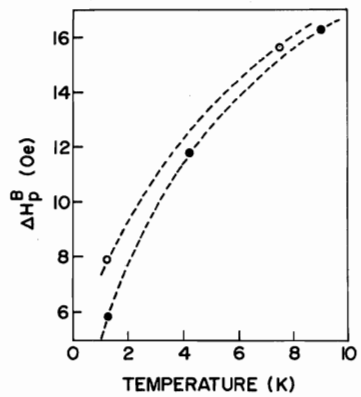

FIG. 9. BCL spin-packet widths as a function of temperature. The slashed lines illustrate a $T^{0.5}$ dependence. Data are plotted for sample 2.2-17 (closed circle) and sample 3.0-17 (open circle).

passage technique.[24] The temperature dependence and magnitudes of the BCL spin-packet widths contrast strongly with the corresponding hyperfine-line results.

(iv) T_1 values: Quantitative measures of the BCL spin-lattice relaxation time T_1^B proved difficult to obtain for our more lightly doped samples ($N_D \leq 1.2\times10^{17}$ donors/cm^3) because of the weak, broad character of the BCL signals in this domain. Strong indications as to the relative relaxation times of the BCL and hyperfine spins were, however, noted. For example, when recovery measurements of T_1^H were made, it was observed that the BCL invariably recovered to its full amplitude even for the shortest available delay time between the successive passages. This behavior is consistent with the inequality $T_1^B < T_1^H$.

The slow-passage saturation method allowed us to determine T_1^B for samples with $N_D \geq 2.2\times10^{17}$ donors/cm^3. Our results are plotted as a function of temperature in Fig. 10 for samples 2.2-17 and 3.0-17, and in both cases T_1^B is roughly proportional to the inverse temperature. A comparison of these data with the corresponding T_1^H results of Fig. 5 indicates that little difference exists between the hyperfine and BCL spin-lattice relaxation rates at the lower end of the experimental temperature range. Above 8 °K it would appear from Figs. 5 and 10 that the hyperfine rates exceed those of the BCL. As noted in Sec. II B, however, this does not indicate that the mean or net spin re-

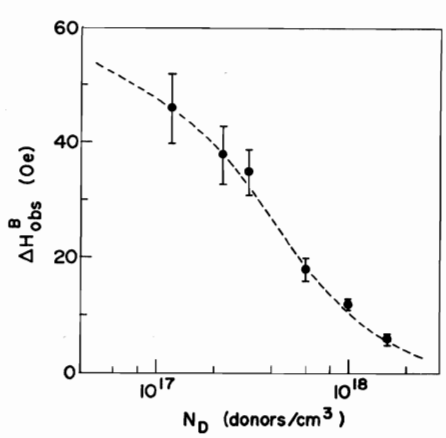

FIG. 8. BCL linewidths as a function of donor concentration (T=1.2 K).

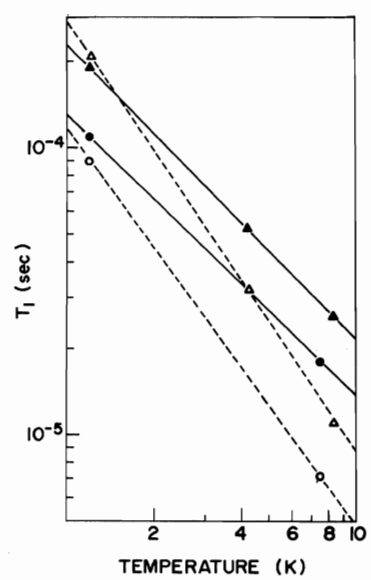

FIG. 10. Experimental BCL spin-lattice relaxation times as a function of temperature for sample 2.2-17 (closed triangle) and sample 3.0-17 (closed circle). The corresponding hyperfine-line spin-lattice relaxation times (open squares and open circles for samples 2.2-17 and 3.0-17, respectively) are included in this figure for comparison purposes.

laxation rate (in the presence of spectral diffusion) of the BCL spins is slower than that of the hyperfine spins.

D. Relative intensities of the spectral components

In the preceding subsections we have presented quantitative measures of the characteristic parameters common to the dominant features of our spectra—the hyperfine and broad center lines. We have so far avoided detailed consideration of the relative intensities of these lines, or, equivalently, of the fractional number of extrinsic spins which contribute to each spectral component. Such an identification is straightforward in the case where all components of the system contribute only slow-passage (unsaturated) signals. A comparison of the area under each of the (decomposed) absorption-envelope components can then be used to find the "fractional susceptibility" associated with each element of the spin system.[25] In particular, the relative susceptibility of the BCL at 1.2 K (χ_s^B/χ_s^{tot}) can be obtained by estimating the fraction of the area under the absorption-envelope spectra of Figs. 2(a), 2(c)–2(f), which is associated only with the BCL. Such an analysis could not be applied to the 1.2-K rapid-passage envelope spectra of sample 1.2-17 because of spectral-diffusion effects which artificially enhance the BCL intensity relative to that of the hyperfine lines.[24] Instead, a measure of this ratio was obtained (utilizing the observed Curie-law dependences of the hyperfine and BCL components) from an (integrated) unsaturated slow-passage absorption-mode signal obtained at 13 °K. Such spectral-diffusion effects could be minimized for sample 5.0-16 and measures of the fractional susceptibility were taken directly from the 1.2-K rapid-passage envelope data. The resulting values of χ_s^B/χ_s^{tot} are plotted as a function of N_D in Figs. 11. It can be observed that the fractional susceptibility of the BCL rises monotonically with N_D through the intermediate concentration range.

The ratios χ_s^B/χ_s^{tot} obtained varied by less than $\pm 5\%$ over the temperature interval $1.2\ \text{K} \lesssim 15$ K for samples with $2.2\times10^{17} < N_D < 6.0\times10^{17}$ donors/cm^3. (As previously noted, the hyperfine lines disappeared at $\simeq 10$ K in sample 1.0-18.) Given the observed Curie-law susceptibility of the hyperfine line, these results would indicate a similar dependence for the BCL spin susceptibility. At temperatures $T \geq 20$ K, these ratios begin to increase appreciably with temperature.

V. DISCUSSION

A. Origin of the EPR spectrum components

In this section we attempt to construct a model of the Si: P system which is consistent with the data of Sec. IV. Such a model must establish a relation between the spatial environment of a given extrinsic spin and the form of its EPR contribution. As indicated in Sec. I, some early success has been achieved in this respect with the identification of the origins of the hyperfine and central lines. The BCL component, on the other hand, has been attributed[10,11] to donor pairs having $J \simeq A$, and to some of the EPR transitions in donor triples.[11,48] The relatively large BCL linewidths are assumed to arise in both cases from the fact that the resonant transition energies depend upon the magnitudes of the donor-donor exchange constants. The random distribution of donors leads to spatial variations in the magnitudes of these exchange constants, giving rise to a single-broad-line EPR spectrum.

In fact, however, the fractional susceptibilities of Fig. 11 are too large to allow the BCL to be understood in terms of the small fraction of donor pairs in which $J \simeq A$. On the other hand, a convincing identification of the BCL as due to clusters of three donors has been hampered by two difficulties. First, the asymmetric BCL shapes previously reported are not easily reproduced by calculations of the cluster-of-three (donor triple) spectrum. This complication has been removed by our results, which indicate a symmetric form for the BCL. A second difficulty remains, however, in that a satisfactory calculation of the donor-triple EPR spectrum has not yet, to our knowledge, been performed. Shimizu[11] has made an attempt in this direction, but his results are inadequate in at least three respects. The most obvious difficulty with his calculated donor-triple spectrum is that it is not invariant under a permutation of the donor spin

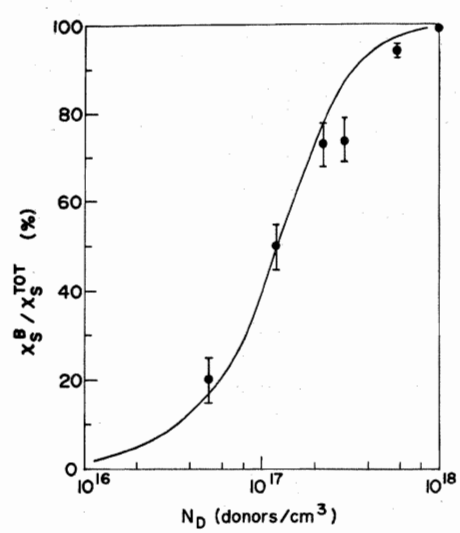

FIG. 11. Relative susceptibility of the BCL spectral component as a function of impurity concentration (T = 1.2 K). The solid curve gives the fraction of donors in clusters of three or more as computed from the results of Holcomb and Rehr (see text).

indices. Second, it predicts significant discrete EPR lines at the resonant fields $H = (1/g_H\mu_B)(\hbar\omega \pm \frac{5}{6}A)$, which have not been observed. A final criticism of this work may be directed at its limitation to energy-level terms which contain A only to the zeroth and first powers. Second-order terms appear to be essential to detailed understanding of the donor-pair spectrum,[8] and we see no reason why this should not also be the case for the donor triple.

We take a somewhat different approach, and note that in any case the donor-triple BCL model will be inadequate for more highly concentrated samples, where significant numbers of higher-order clusters (i.e., of four, five, etc., donors) may be expected. To account for this circumstance it is useful to employ the results of the Holcomb and Rehr[49] Monte Carlo calculation to obtain the probability P_3 ($\equiv N_3/N_D$) that a given donor is a member of a cluster of three *or more* impurity atoms. In this model the cluster membership criterion requires that a member donor must be separated from at least one other member of the cluster by less than a maximum distance R_{max}. The solid line in Fig. 11 is a plot of N_3/N_D for a particular value of R_{max} ($R_{max} = 132 \pm 6$ Å) which was chosen to optimize the agreement between N_3/N_D and χ_s^B/χ_s^{tot}. This agreement is seen to be quite good except, perhaps, for samples with impurity concentrations near the upper end of the intermediate range, where the relative BCL susceptibility does not increase quite as rapidly as N_3/N_D. Further, the 132-Å value obtained for R_{max} is consistent with expectations[50] on the basis of our earlier study of interdonor interactions.[10,39] We therefore feel that the correspondence of N_3/N_D and χ_s^B/χ_s^{tot} illustrated in Fig. 11 provides considerable support for the proposal that the BCL arises primarily from clusters of three or more donors.

This proposal is similar in some respects to a hypothesis offered previously by Morigaki and Maekawa.[17] The specifics of their model are discussed in the following subsections in connection with our g-value and spin-relaxation data.

B. Discussion of g-value measurements

In Sec. IV important differences were noted between the g values associated with the BCL and hyperfine lines, respectively. The BCL g values g_B decrease toward the conduction-electron g value g_e as the temperature is raised from 1.1 K and/or as the impurity concentration is increased through the interval $1\times10^{17} \le N_D \le 2\times10^{18}$ donors/cm^3. The hyperfine-line g value g_H, on the other hand, is temperature independent and falls below g_e when the concentration is increased above $N_D \sim 1\times10^{17}$ donors/cm^3.

Morigaki and Maekawa[17] have attempted to explain the BCL g shifts in terms of an "effective-field" approximation which entails a ferromagnetic exchange interaction between neighboring clusters. The interdonor coupling within a cluster was still assumed to be of the usual antiferromagnetic form and the predicted g-value shift written as[18]

$$g_B - g_e = -f\mathfrak{F}/kT \ . \tag{9}$$

In this expression f is a constant related to the number of spins in a given cluster and $\mathfrak{F}$ is an average exchange constant descriptive of the intercluster coupling. This latter quantity must be negative (ferromagnetic) in order to account for the positive experimental values of $g_B - g_e$.

If we assume that f and $\mathfrak{F}$ are temperature independent, Eq. (9) offers a reasonably good description of the experimentally observed temperature dependence of g_B. The observed concentration dependence, however, requires that the product $f\mathfrak{F}$ be a decreasing function of the impurity concentration when $N_D \gtrsim 2\times10^{17}$ donors/cm^3. It is possible that such behavior could arise from a decrease in the importance of intercluster coupling as the average size of the clusters is increased. There is, however, no other independent evidence for such an effect. Completeness, within such a model, would also appear to require that $g_B - g_e$ tends to zero at low impurity concentrations where large cluster separations may be expected to give negligible ferromagnetic coupling. Unfortunately, the amplitude and width of the BCL signals in samples with $N_D \lesssim 1.2\times10^{17}$ donors/cm^3 are such that g-value measurements cannot be made to sufficient accuracy to check this hypothesis.

Perhaps the most sensitive detectors of the internal effective fields postulated in the Morigaki-Maekawa[17] model would be the highly coupled donor-pair spin transitions which contribute to the hyperfine and central-pair EPR lines. These pair transitions may be expected to respond in a similar manner to the effective fields associated with the intercluster coupling and contribute an appreciable fraction of the observed hyperfine-line intensity in our more highly concentrated samples. The g shifts $g_H - g_e$ of the hyperfine lines in such samples can therefore be used to test the Morigaki-Maekawa model. However in this case the observed g-value shifts would indicate that $\mathfrak{F} > 0$ and that $f\mathfrak{F}$ increases with increasing N_D. These conclusions conflict with the results previously inferred from the BCL data. Further, the observed temperature independence of g_H is inexplicable in terms of a relationship similar to Eq. (9). We therefore conclude that the observed behavior of g_H is not consistent with the Morigaki-Maekawa model of the BCL.

We believe that a better understanding of the shifts observed in the position of the BCL may be

achieved in terms of a more complete calculation of the donor-triple spectrum. An indication of this possibility may be found in the fact that the deviations $g_B - g_e$ exhibit behavior, as a function of N_D and T, very similar to that noted earlier [see Sec. IV A (ii) for $g_c - g_e$]. The latter shifts are apparently explicable in terms of the second-order J-dependent energy-level scheme, and hence an equivalent shifting mechanism would appear likely to exist in the case of the donor triples and larger clusters, which, according to our thesis, are the dominant sources of the BCL.

The observed concentration dependence of g_B may be attributed to the enhanced electron delocalization which obtains in the increasingly large clusters which appear as N_D is raised to 2×10^{18} donors/cm^3. In large enough clusters, the collective behavior of the extrinsic electrons will produce shielding effects that reduce the attractive potential of any particular impurity site in that cluster. In the limit of total shielding (no hyperfine interaction) we expect to monitor a single EPR line with the "free"-electron g value g_e. In this view, the shift of g_B towards g_e with rising N_D reflects the increasingly delocalized nature of the extrinsic electrons responsible for the BCL.

The observed shift in hyperfine-line position indicated by the concentration dependence of g_H would appear to be a phenomenon entirely distinct from the expected shifts due to the second-order (in A) terms in the donor-pair transitions which occur at or near the hyperfine-line frequencies.[51] Our only explanation for this result must be based on the ideas of Sec. V C, in which it is argued that the isolated (hyperfine line) spins relax via cross relaxation to the faster relaxing clusters associated with the BCL. Some of the allowed transitions corresponding to clusters of three and four donors occur at or near the hyperfine-line frequencies, and it is these transitions which may be responsible for significant cross-relaxation effects. If these transition frequencies are appreciably shifted by second-order effects similar to those predicted for the donor pair, we may expect the hyperfine lines to exhibit a similar shift. This is, of course, providing the cluster transition is still within $1/T_2^H$ of the original hyperfine-line resonant frequency, and the intrinsic hyperfine spin relaxation rates are slower than those associated with cross relaxation. Such a mechanism would also be temperature independent within the above limitations.

C. Linewidths and relaxation times

In this section we first discuss the spin-packet width and spin-lattice relaxation-time data pertaining to both the BCL and hyperfine lines. Subsequently, a model is suggested whereby (isolated) spins contributing to the hyperfine lines relax to the lattice via intermediary "cross-relaxation" processes[52] with faster-relaxing BCL spins. It is shown that this model would account for the observed concentration and temperature dependences of the hyperfine spin-lattice relaxation time T_1^H.

The magnitudes of the hyperfine-line spin-packet widths appreciably exceed those values inferred from either spin-lifetime calculations[53] (assuming dipolar spin-spin coupling) or early measurements of the decay rate of spin echoes.[42] The concentration dependence $\Delta H_P^H \propto N_D^{2.5}$, which was observed over most of the intermediate range, is also in strong disagreement with the concentration independence of the spin-echo results.[42] These discrepancies have been substantially resolved by a recent publication,[54] where it is argued that the spin-echo experiments in question give an incorrect measure of the spin-spin interactions appropriate to our EPR experiments. The large spin-packet widths observed, and the correspondingly fast spin-echo decays obtained in recent pulse experiments[54] can both be understood in terms of interdonor exchange interactions. (Even in a sample as dilute as $N_D = 5\times10^{16}$ donors/cm^3 approximately 80% of all donors have a nearest neighbor close enough to realize an exchange interaction $J \gtrsim \gamma\Delta H_P^H$.)

The BCL packet widths exhibit a strong concentration dependence similar to that observed for ΔH_P^H. This dependence may be qualitatively understood in terms of previously discussed[30] exchange-narrowing arguments. Using the earlier notation,[30] it may be observed that the exchange interaction J between nearby effective spins A and B will eventually exceed $\Delta\omega_{AB}/2\pi$ as N_D is increased. This results in the formation of a new "exchange-narrowed" effective spin with resonant frequency $(\omega_A + \omega_B)/4\pi$. The observed increase of the experimental packet width toward the observed linewidth, as N_D is increased, indicates that we observe the response of progressively larger clusters or effective spins, until the limiting high-concentration case is reached where all donors in the sample may be considered to constitute a single large cluster.

The hyperfine spin-lattice relaxation-time (T_1^H) data of Fig. 4 illustrated the dominance of concentration-dependent (extrinsic) spin relaxation mechanisms in our intermediately doped Si : P samples. As indicated by earlier work,[15] the rather weak T_1^H concentration dependence $[T_1^H \propto (N_D)^{-3/2}]$ observed for samples with $N_D \leq 4\times10^{16}$ donors/cm^3 becomes considerably stronger at larger impurity concentrations. By way of example, the approximately fourfold increase of N_D between samples 5.0-16 and 2.2-17 results, at 1.2 K, in a reduction of T_1^H by a factor of approximately 10^6. In view of these large changes in the relaxation rates we found it surprising that the low-temperature

$T_1^H \propto T^{-3/2}$ dependence observed in dilute samples[44] was obeyed throughout the rest of the intermediate range. This continuity would, at first glance, appear to have important implications for the fast-center models previously proposed[9] to explain the T_1^H data. In these models it is assumed that most of the "isolated" donors (which, for $N_D < 6\times10^{17}$ donors/cm^3, contribute the major portion of the observed hyperfine-line intensity) relax to the lattice through a process which involves spatial spin diffusion and cross relaxation with fast-relaxing centers. The Yang-Honig[9] treatment of earlier Si : P EPR data assumes the fast-relaxing centers (FRC's) to be strongly coupled donor pairs. Fast relaxation rates in such pairs have been observed experimentally[9,24] and are consistent with theoretical expectations.[12] Since the (pair) exchange interaction is diagonal in the total electronic spin, however, the pair relaxation mechanism is dependent upon a mixing (by the hyperfine interaction) of states of different electronic spin. This mixing requirement is responsible for a considerable reduction in the size of the transition matrix elements relative to those associated with the donor triple. In the latter case a simple modulation of the isotropic exchange interaction by the lattice vibrations can directly induce spin relaxation.[55] We may therefore expect that a cluster of $n \geq 3$ donors would relax to the lattice at a rate significantly faster than that of a pair, assuming comparable interdonor separations. This expectation is consistent with our BCL T_1^B data, and our proposal that this line arises from clusters of three or more donors. The continuity of the $T_1^H \propto T^{-3/2}$ dependence through the intermediate concentration range cannot, however, be used to justify the dominance of a donor-triple FRC mechanism in all of these samples. It is possible, however, to contend that the stronger concentration dependence of T_1^H, observed when N_D exceeds $\sim 5\times10^{16}$ donors/cm^3, is due to the increasing availability of donor-triple FRC's. In any case a fairly strong argument may be made for a model in which the spin in the BCL serve as fast-relaxing centers for the more isolated hyperfine-line centers. This proposal is discussed in the following paragraphs.

First, in order to qualify as fast centers, the BCL spins must have spin relaxation rates which are significantly faster than those of the isolated spins contributing to the hyperfine lines. Our experimental results would, at first glance, appear to present some difficulties in this respect since it was observed that T_1^B may exceed T_1^H in samples with $N_D \geq 2.2\times10^{17}$ donors/cm^3. As noted in Sec. II B, however, the relevant spin-relaxation parameter is the mean or net spin relaxation rate $1/\tau$ defined in Eq. (2). Assuming that $T_3 < T_1$ (which was satisfied in all experimental situations), the relevant fast-center BCL criterion is that $T_3^B < T_3^H$. It was found that this inequality was satisfied by at least an order of magnitude for all slow-passage samples. This experimental fact can therefore be taken as evidence for the fast-relaxing-center capability of the BCL spins.

In the past, the possibility of significant spin relaxation through donor-triple FRC's has been neglected in samples with $N_D \lesssim 5\times10^{16}$ donors/cm^3, since the number of such clusters was assumed to be very small. However, on the basis of our cluster-membership criterion, it would appear that even in a 3×10^{16} donors/cm^3 sample approximately 5% of all donors belong to clusters of three or more impurities. Assuming that the BCL packet widths are large enough to allow good cross-relaxation contact between the isolated hyperfine spins and the BCL spins (as evidenced by the strong spectral-diffusion effects, evidently responsible for off-line saturation EPR phenomena[19,24]) we contend that donor triples must be considered as competitive fast centers for concentrations as low as 1×10^{16} donors/cm^3.

The relaxation of the isolated spins may then be qualitatively understood in terms of the Yang-Honig fast-center model, where the fast centers are the BCL spins. Given that $T_3^H \ll T_1^H$ in all cases, isolated spins will experience relatively rapid spectral diffusion until they encounter an FRC with which they can cross relax. Assuming that the cross-relaxation time is much shorter than the BCL fast-center spin-lattice relaxation time, the extrinsic spin-lattice relaxation rate of the isolated spins will obey the proportionality[56]

$$\frac{1}{T_1^H} \propto \frac{N_{\rm FRC}}{N_H}\,\frac{1}{T_R^{\rm FRC}}\,, \tag{10}$$

where $N_{\rm FRC}$ is the number of BCL fast centers available to a given isolated spin, and N_H is the number of isolated spins. $T_R^{\rm FRC}$ is the spin relaxation time of the BCL fast centers. The quantity $N_{\rm FRC}$ appropriate to a hyperfine-line spin at a resonant field $H = H'$ would be expected to be fairly well given by the number of BCL spins in the packet of width ΔH_P^B centered at H'. As $\Delta H_{\rm obs}^B$ changes only a small amount with increasing temperature for $T \leq 10$ K, $N_{\rm FRC}$ would be proportional to ΔH_P^B. The identification of $T_R^{\rm FRC}$ with either T_1^B or T_3^B depends on the degree to which the BCL spin system is saturated by the microwave radiation, as discussed in Section II B. Given that $T_3^B < T_1^B$, and saturation (rapid passage) conditions, the fast-center relaxation time would be given by $T_R^{\rm FRC} = T_1^B$. The experimental proportionalities $T_1^B \propto T^{-1}$, $\Delta H_P^B \propto T^{0.5}$ and the assumption $N_{\rm FRC} \propto \Delta H_P^B$ when substituted into Eq. (10) lead to the relation $T_1^H \propto T^{-1.5}$, in agreement with the results in rapid-passage situations. Under nonsaturating slow-passage

conditions, however, T_3^B describes the time taken for a spin to relax to the lattice temperature and is, therefore, the effective spin-lattice relaxation time. Identifying $T_R^{FRC} = T_3^B = (T_1^B T_2^B/a)^{1/2}$, where $a = \Delta H_P^B/\Delta H_G^B \simeq \Delta H_P^B/\Delta H_{obs}^B$ $(a<1)$, we obtain $T_R^{FRC} \propto T^{-1}$, which leads to the same $T_1^H \propto T^{-1.5}$ relation obtained in the rapid-passage case, and is in agreement with our slow-passage experimental results. It is impossible, however, to predict the concentration dependence and magnitudes of T_1^H in terms of this model in the absence of a detailed expression for the fast-center relaxation rate. Further progress in understanding these concentration-dependent spin-lattice processes would appear to require further theoretical studies of BCL and hyperfine line-shape and relaxation parameters.

D. Summary

The primary aim of this work has been to clarify the nature of the EPR spectra peculiar to Si : P samples with intermediate impurity concentrations. As most of the difficulties previously encountered have concerned the "broad background" or "broad center" line (BCL), much of our attention has been devoted to this spectral component. This line is observed to be of the standard symmetric form associated with a convolution of a Gaussian envelope with Lorentzian spin-packet contributions. Its behavior, with regard to field position and linewidth as the impurity concentration and/or temperature is raised, confirms that it is the low-concentration percursor of the single EPR line seen in samples with $N_D \gtrsim 2\times 10^{18}$ donors/cm^3.

Our measurements reveal that the relative susceptibility of this line correlates well with the expected fraction of donors which exist as members of clusters of three or more impurity atoms. The observed variation of BCL and hyperfine-line parameters do not seem inconsistent with the anticipated results of a second-order calculation of the EPR spectrum of a cluster of three donors.

The observed intensities, spin relaxation rates and spin-packet widths associated with the BCL suggest that clusters contributing to the BCL may serve as important fast-relaxing centers for the relatively isolated "hyperfine" spins, even in relatively dilute samples. A simple mechanism is suggested for this relaxation process based on a correspondence between the number of effective BCL fast centers and the width of the BCL spin packets. Insufficient understanding of both spin-spin and spin-lattice interactions do not presently allow verification of this model or its extension to a more quantitative form.

ACKNOWLEDGMENTS

We would like to thank Dr. D.D. Thornton, now of George Washington University, for his participation in the early stages of this work. We are also grateful to Dr. C. Mailer, of the University of Western Ontario, for calling several important references to our attention.

APPENDIX: EXTENSION OF THE CASTNER SATURATION-CURVE CALCULATION

An integral form of the inhomogeneously broadened absorption-envelope line shape was derived by Castner,[22] assuming a Gaussian envelope and Lorentzian spin packets, and can be written as

$$\chi''(H) = \frac{\chi_0}{2\pi^{1/2}\Delta H_P'\Delta H_G'} \times \int_0^\infty \frac{H' e^{-[(H'-H_0)/\Delta H_G']^2}\, dH'}{1+[(H'-H_0)/\Delta H_P']^2 + \gamma^2 H_1^2 T_1 T_2}, \tag{A1}$$

where $\Delta H_P' = \Delta H_P/2$ and $\Delta H_G' = \Delta H_G/1.665$. We identify ΔH_P as the full spin-packet width at half-maximum, ΔH_G as the full Gaussian-envelope width at half-maximum, and χ_0 as the "static" magnetic susceptibility. Letting $S^2 = 1+\gamma^2 H_1^2 T_1 T_2$, $y = (H'-H_0)/\Delta H_G'$, $a = \Delta H_P'/\Delta H_G'$ and $v = (H-H_0)/\Delta H_G'$, and noting that H' varies slowly in comparison with other terms in the integrand of Eq. (A1)$(H_0 \gg \Delta H_P, \Delta H_G)$, we obtain

$$\chi''(H) = \frac{\chi_0 H}{\pi^{1/2}\Delta H_G'} \frac{1}{s}\left[b \int \frac{e^{-y^2}}{b^2+(v-y)^2}\, dy \right], \tag{A2}$$

where $b = as$. At the line center $v=0$, and it is easy to obtain the Castner saturation-curve result[22]

$$\chi''(H_0) = \frac{\chi_0 H_0}{\Delta H_G} \frac{e^{a^2 s^2}[1-\mathrm{erf}(as)]}{s}. \tag{A3}$$

The parameters a and $(T_1T_2)^{1/2}$ may be obtained in the manner described by Castner.[22]

The Gaussian half-width ΔH_G is not necessarily equal to the width of the experimentally observed line. Given low microwave power so that the spin system is not saturated (i.e., $s=1$), we have

$$\chi''(H) = \frac{\chi_0 H}{\pi^{1/2}\Delta H_G'} \left[a \int \frac{e^{-y^2}}{a^2+(v-y)^2} dy \right]. \tag{A4}$$

The term in brackets is commonly called a Voigt profile. Posener[57] has determined the observed half-width at half-amplitude (ΔH_{obs}) of this profile as a function of a, and has shown that ΔH_{obs} is related to the Gaussian half-width according to

$$\Delta H_{obs} = w\,\Delta H_G/0.832, \tag{A5}$$

where the correction factor w is a computed function of a. It is easy to show that the spin-packet width is related to ΔH_{obs} according to

$$\Delta H_P = (a/w)\Delta H_{obs} \tag{A6}$$

when $a \gg 1$, $w \simeq a$, and therefore $\Delta H_P = \Delta H_{obs}$ in such situations.

*Research supported by Grant No. 67-4624 from the National Research Council of Canada.

†Now at the Biochemistry Department, South Parks Road, Oxford, England.

‡Present address: Marine Sciences Directorate, Environment Canada, 512-1230 Government Street, Victoria, British Columbia, Canada.

[1]Reviews of the earlier work in this field have been contributed by Ludwig and Woodbury, in *Solid State Physics*, edited by F. Seitz and D. Turnbull (Academic, New York, 1963), Vol. 13; G. F. Lancaster, *Electron Spin Resonance in Semiconductors* (Hilger and Watts, London, 1966).

[2]J. D. Quirt and J. R. Marko, Phys. Rev. Lett. 26, 318 (1971).

[3]H. Ue and S. Maekawa, Phys. Rev. B 3, 4232 (1971).

[4]J. D. Quirt and J. R. Marko, Phys. Rev. B 5, 1716 (1972).

[5]J. D. Quirt and J. R. Marko, Phys. Rev. B 7, 3842 (1973).

[6]C. P. Slichter, Phys. Rev. 99, 479 (1955).

[7]E. Sonder and H. C. Schweinler, Phys. Rev. 117, 1216 (1960).

[8]D. Jerome and J. M. Winter, Phys. Rev. 134, A1001 (1964).

[9]G. Yang and A. Honig, Phys. Rev. 168, 271 (1968).

[10]J. R. Marko, Phys. Lett. A 27, 119 (1968).

[11]T. Shimizu, J. Phys. Soc. Jap. 25, 1021 (1968).

[12]J. R. Marko, Can. J. Phys. 48, 834 (1970).

[13]V. Macek, Ph.D. thesis (University of British Columbia, 1971) (unpublished).

[14]G. Feher, R. C. Fletcher, and E. A. Gere, Phys. Rev. 100, 1784 (1955).

[15]G. Feher and E. A. Gere, Phys. Rev. 114, 1245 (1959).

[16]A. Honig, in *Quantum Electronics*, edited by C. H. Townes (Columbia U.P., New York, 1960), p. 450.

[17]K. Morigaki and S. Maekawa, J. Phys. Soc. Jap. 32 (1972). Earlier versions of this work have appeared in Proceedings of the International Conference on Semiconductors, Moscow, 1968, p. 1126 (unpublished), and J. Phys. Soc. Jap. 25, 912 (1968).

[18]In Ref. 17, our effective g shifts were referred to as shifts in the resonance field. The two descriptions are equivalent.

[19]G. Feher, Phys. Rev. 114, 1219 (1959). In this work the inhomogeneously broadened nature of EPR responses from Si:P EPR signals at low temperatures and impurity concentration was first noted. It was shown that the 4.8%-abundant Si^{29} isotope is chiefly responsible for this inhomogeneous broadening, at least for samples with $N_D \lesssim 3\times 10^{16}$ donors/cm^3.

[20]F. Bloch, Phys. Rev. 70, 460 (1946).

[21]A. M. Portis, Phys. Rev. 91, 1071 (1953).

[22]T. G. Castner, Jr., Phys. Rev. 115, 1506 (1959).

[23]A. M. Stoneham, Rev. Mod. Phys. 41, 82 (1969).

[24]P. R. Cullis, Ph.D. thesis (University of British Columbia, 1972) (unpublished).

[25]W. Voight and S. B. Bayer, Akad. Wiss. 1912, 603 (1912).

[26]E. L. Wolf, Phys. Rev. 142, 555 (1966).

[27]S. Clough and C. A. Scott, J. Phys. Chem. (Proc. Phys. Soc.) 1, 919 (1968).

[28]J. R. Klauder and P. W. Anderson, Phys. Rev. 125, 912 (1962).

[29]P. W. Anderson, Phys. Rev. 82, 342 (1951); C. Kittel and E. Abrahams, Phys. Rev. 90, 238 (1953).

[30]P. W. Anderson, J. Phys. Soc. Jap. 9, 316 (1954). In this work Anderson shows that if the splitting between a pair of exchange-coupled spins A and B is written as $\Delta\omega_{AB} = |\omega_A - \omega_B|$, and the exchange interaction $J < \Delta\omega_{AB}/2\pi$, the two spectral lines corresponding to A and B remain Lorentzian but are somewhat broadened (exchange broadening). If, on the other hand, $J > \Delta\omega_{AB}/2\pi$, the lines draw closer together to form, in the $J >> \Delta\omega_{AB}/2\pi$ limit, a single exchange-narrowed resonance line which has the form of a cut-off Lorentzian. The only case in which the dominant response is not Lorentzian is when $J \approx \omega_{AB}/2\pi$. In the case of Si:P the latter condition would be satisfied for only a negligibly small fraction of the electronic spins in the randomly distributed donor system.

[31]A. M. Portis, Technical Note No. 1, Sarah Mellon Scaife Radiation Laboratory, University of Pittsburgh, 1955 (unpublished).

[32]A. A. Bugai, Fiz. Tverd. Tela 4, 3027 (1962) [Sov. Phys.-Solid State 4, 2218 (1963)].

[33]T. H. Wilmshurst, *Electron Spin Resonance Spectrometers* (Adam Hilger, London, 1967).

[34]L. E. Drain, Proc. Phys. Soc. Lond, A 62, 301 (1949).

[35]Castner (Ref. 22) assumes that the half-width of the experimentally observed Voigt profile (ΔH_{obs}) is equal to the width of the Gaussian envelope ΔH_G. This is not the case for $\Delta H_p \gtrsim \Delta H_G$, since it gives the unphysical result that the spin-packet half-width is greater than ΔH_{obs} for situations in which the inhomogeneity parameter a ($= \Delta H_p/\Delta H_G$) is greater than 1. As shown in the Appendix, however, the Voigt-profile half-width is actually related to the spin-packet width ΔH_p according to $\Delta H_p = (a/w)\ \Delta H_{obs}$, where w is a correction factor which, when $a \gg 1$, becomes approximately equal to a. This gives the more appealing result that the spin-packet width in the "homogeneous" limit is equal to the half-width of the experimentally observed line.

[36]S. Maekawa and N. Kinoshita, J. Phys. Soc. Jap. 20, 1447 (1965).

[37]H. Kodera, J. Phys. Soc. Jap. 27 1197 (1969).

[38]The central line is associated with the following transitions in the pair-spin-level structure: (i) $|T_1, t_0> \longleftrightarrow |T_0, t_0>$; (ii) $|T_1, s> \longleftrightarrow T_0, s>$; (iii) $|T_0, t_0> \longleftrightarrow |T_{-1}, t_0>$; (iv) $|T_{-1}, t_0> \longleftrightarrow |T_{-1}, s>$, where symbols T (t) and S (s) refer, respectively, to the triplet and singlet electronic (nuclear) spin states. [The subscripts attached to these symbols indicate the components of these spins along the z direction (parallel to H).] At low enough temperatures the states involved in transitions (i) and (ii) become thermally depopulated and, in this limit, the central-line intensity arises largely from transitions (iii) and (iv). Using the energy levels calculated (Ref. 8) to second order in A, we find that the latter pair of transitions occur at a resonant field which (assuming $h\omega >> J$) lies $\approx A^2J/4g\mu_B$ below the midpoint of the "isolated" hyperfine-line spectrum. This would account for the anomalous displacement of the central line at low temperatures. Furthermore, since transitions (i) and (ii) correspond to resonant fields displaced by $+A^2J/4g\mu_B$ from the hyperfine-spectrum midpoint, one would expect the increased contributions from these transitions with rising temperature to eliminate the anomalous shift of the slightly

broadened central line. Such an effect has been observed in our experiments, where no difference in the positions of the central line and the hyperfine-spectrum midpoint can be detected for $T > 4.2$ K. Our measured shift at 1.1 K corresponds to an average pair exchange constant $J \sim 6A$.

[39]P. R. Cullis and J. R. Marko, Phys. Rev. B 1, 632 (1970).

[40]D. J. Lepine, Phys. Rev. B 2, 2429 (1970).

[41]Within the accuracy of our measurements the hyperfine splitting was not observed to vary over the intermediate range and the quoted value of A is the mean value of these measurements. The discrepancy between our value of A and that due to Feher (Ref. 19) ($A = 42.0$ Oe) for a sample with $N_D = 5 \times 10^{16}$ donors/cm^3 may reflect a very slight decrease of the hyperfine splitting with increasing impurity concentration. In this regard H. Kodera [J. Phys. Soc. Jap. 27, 1197 (1969)] obtains $A = 41.7 \pm 0.6$ Oe for samples with impurity concentrations in the middle of the intermediate range.

[42]J. P. Gordon and K. D. Bowers, Phys. Rev. Lett. 1, 368 (1958).

[43]T. G. Castner, Jr., Phys. Rev. 130, 58 (1963).

[44]It is important to note that although discrepancies were found between the T_1's obtained by the alternative rapid- and slow-passage techniques in samples 2.2-17, both sets of data were consistent with the noted $T_1^H \propto T^{-3/2}$ law.

[45]J. R. Marko and A. Honig, Solid State Commun. 8, 1639 (1970).

[46]Asymmetric line shapes similar to those reported in Ref. 17 were observed when the spectrometer was operated in the slow-passage dispersive ($d\chi'/dH$) signal mode. However, it was found that the senses of these asymmetries were dependent upon the location of the klystron frequency with respect to the cavity absorption "dip" in the reflected klystron power. This was interpreted as a result of the change in the dispersive-signal polarity when the klystron frequency is shifted from one side of this dip to the other. Since the sign of any remnant absorptive signal component is invariant to this frequency change, it results in a change in the relative polarities of the two signal components and thus gives rise to spectrometer-tuning-dependent asymmetries.

[47]Some of the discrepancies between the data presented here and in Ref. 17 may be attributed to the different methods used to establish the sample impurity concentrations. On the basis of previously offered arguments (Ref. 5), we believe that the N_D values quoted by Morigaki and Maekawa may be lower than the actual impurity concentrations in these samples by nearly a factor of 2.

[48]A. Abragam (unpublished notes).

[49]D. F. Holcomb and J. J. Rehr, Phys. Rev. 183, 773 (1969).

[50]Using the previously determined relationship (Ref. 39) between the exchange constant J and the interdonor separation r, R_{max} corresponds to a minimum interaction $J_{min} \simeq 0.4A$ ($A = 118$ MHz). This minimum interaction criterion for cluster membership is reasonable in view of the pair-spectrum results (Refs. 10 and 39) and the changes which might be expected when such considerations are extended to higher-order clusters.

[51]These effects can be illustrated by specific reference to the second-order pair calculation of Jerome and Winter (Ref. 8). These authors observed that the pair transitions at the hyperfine-line frequencies are shifted to higher fields (or lower g value) by an amount on the order of $A^2/4\nu_e$ ($= 0.14$ Oe), where ν_e is the resonant frequency of the "free" electron. Further, one of the components contributing to the high-frequency hyperfine line is shifted to a yet higher field by an exchange-dependent amount, $A^2/4(\nu_e - J)$ (for $J < \nu_e$). This particular second-order effect would be consistent with the observed shift of g_H to lower values as N_D is raised, except that it is too small. Also, of course, we observe equivalent shifting of both the high- and low-field hyperfine lines according to the values of g_H quoted in Fig. 3.

[52]N. Bloembergen, S. Shapiro, P. S. Pershan, and J. O. Artman, Phys. Rev. 114, 445 (1959).

[53]A. M. Portis, Phys. Rev. 104, 584 (1956).

[54]D. R. Taylor, J. R. Marko and I. G. Bartlett, Solid State Commun. 14, 295 (1974).

[55]E. A. Horris and K. S. Yngresson, J. Phys. C 1, 990 (1968).

[56]The authors are grateful to the referee for pointing out an inconsistency in their original formulation of Eq. (10).

[57]D. W. Posener, Aust. J. Phys. 12, 184 (1959).